Preparation and Performance of Pd Particles Encapsulated in Block Copolymer Nanospheres as a Hydrogenation Catalyst

Royale S. Underhill and Guojun Liu*

Department of Chemistry, University of Calgary, 2500 University Drive, NW, Calgary, Alberta, Canada T2N 1N4

Received July 17, 2000. Revised Manuscript Received September 13, 2000

Triblock nanospheres with hydroxylated polyisoprene (PHI) coronas, cross-linked poly(2-cinnamoyloxyethyl methacrylate) shells, and poly(acrylic acid) (PAA) cores were prepared following a method described previously. Equilibrating such nanospheres with a $PdCl_2$ solution in methanol enabled the loading of Pd^{2+} into the PAA cores of the nanospheres. After the excess $PdCl_2$ in the methanol phase was removed, Pd(II) inside the nanosphere cores was reduced with hydrazine to yield Pd nanoparticles. Such encapsulated Pd particles were dispersed in methanol or water, which solubilized PHI. Like Pd black, the nanosphere-encapsulated Pd nanoparticles catalyzed the hydrogenation of alkenes. The need for the reactant(s) to diffuse into and products to diffuse out of the encapsulating nanospheres expectedly slowed the catalytic reactions. The more interesting aspect had been in our ability to modify the activity of the Pd catalyst via changing the pH and thus the conformation of the encapsulating polymer chains.

Introduction

In this paper, we report the preparation of palladium (Pd) nanoparticles encapsulated in triblock copolymer nanosphere cores. The nanospheres were prepared following a method reported previously.[1] They have hydroxylated polyisoprene (PHI) coronas, cross-linked poly(2-cinnamoyloxyethyl methacrylate) (PCEMA) shells, and poly(acrylic acid) (PAA) cores. Pd nanoparticles were obtained following the procedures of Scheme 1.

Also reported in this paper is the performance of these Pd particles as a catalyst for the hydrogenation of alkenes.

The use of triblock nanospheres as the templates for Pd or metal particle formation has never been reported. The closest case would be the use of diblock micelles for such purposes as exemplified by the work of Spatz et al.[2] and of Antonietti and co-workers.[3,4] Alternatively, palladium or other metal nanoclusters have been prepared in the cores of dendrimers.[5−7] More simply, they can be prepared in a solvent by reducing Pd salt in the presence of a polymer[8−10] or a small-molecule ligand[11−14] as the dispersing agent. Palladium and other metal nanoclusters have also been prepared in the domains of block-segregated diblock bulk,[15] in the matrix of a homopolymer,[16] in zeolite cavities,[17] in mesoporous silica films,[18] and in silica particles prepared from microemulsion processes.[19] As will be evident later, the distinct advantage for preparing Pd nanoparticles in the core of triblock nanospheres is that this is a templated synthesis and that size of the Pd particles prepared are smaller than that of the core of the nanospheres. The drawback is the cost associated with the production of such nanospheres.

Scheme 1. Schematic Illustration of the Procedures Used for Preparing Nanosphere-Encapsulated Pd Particles [Equilibrating the Nanospheres with a $PdCl_2$ Solution in Methanol Enabled the Loading of Pd^{2+} into the PAA Cores of the Nanospheres (Red to Gray); Pd Nanoparticles Were Obtained by Reducing Pd^{2+} inside the Nanosphere Cores with Hydrazine (Black Domain Formation)]

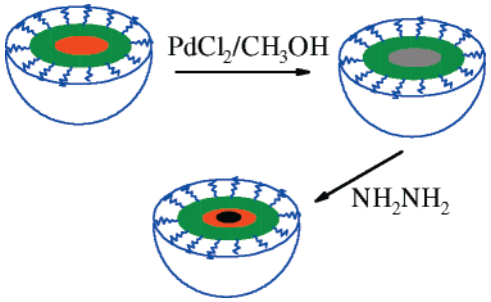

Experimental Section

Palladium Loading. For monitoring the kinetics of $PdCl_2$ entrance into the cores of the nanospheres, 100 mg of nano-

(1) Underhill, R. S.; Liu, G. *Chem. Mater.* **2000**, *12*, 2082−2091.
(2) Spatz, J. P.; Roescher, A.; Sheiko, S.; Krausch, G.; Moller, M. *Adv. Mater.* **1995**, *7*, 1000.
(3) (a) Antonietti, M.; Wenz, E.; Bronstein, L.; Seregina, M. *Adv. Mater.* **1995**, *7*, 1000. (b) Klingelhofer, S.; Heitz, W.; Greiner, A.; Oestreich, S.; Forster, S.; Antonietti, M. *J. Am. Chem. Soc.* **1997**, *119*, 10116. (c) Seregina, M. V.; Bronstein, L. M.; Platonova, O. A.; Chernyshov, D. M.; Valetsky, P. M.; Hartmann, J.; Wenz, E.; Antonietti. M. *Chem. Mater.* **1997**, *9*, 932.
(4) Forster, S.; Antonietti, M. *Adv. Mater.* **1998**, *10*, 195.
(5) Balogh, L.; Tomalia, D. A. *J. Am. Chem. Soc.* **1998**, *120*, 7355.
(6) (a) Zhao, M.; Sun, L.; Crooks, R. M. *J. Am. Chem. Soc.* **1998**, *120*, 4877. (b) Zhao, M.; Crooks, R. M. *Angew. Chem., Int. Ed.* **1999**, *38*, 364.
(7) Vassilev, K.; Kreider, J.; Miller, P. D.; Ford, W. T. *React. Funct. Polym.* **1999**, *41*, 205.

10.1021/cm0005743 CCC: $19.00
Published on Web 11/16/2000

spheres were dissolved in 50 mL of methanol purged with argon. To it was added $PdCl_2$ (0.1884 g; 3.3 mol equivalent to AA) dissolved in 50 mL of methanol purged with argon. Aliquots, at 5 mL, were taken at 5, 10, 20, and 40 min and then 1, 4, 8, 12, 24, and 48 h. The aliquots were centrifuged for 5 min at 14 000 rpm to settle the nanospheres, which were subsequently washed three times, at 10 min each time, with 0.01 N HCl to remove excess Pd^{2+}, which might have been on the outside of the nanospheres. The nanospheres were then dried under vacuum overnight. Once dry they were analyzed for $PdCl_2$ content using thermogravimetric analysis (TGA).

For producing Pd particles encapsulated in nanospheres, the nanospheres were equilibrated with $PdCl_2$ for 48 h. After the exterior Pd^{2+} was removed following the same procedure described above, the nanospheres were redispersed in water. To it 10% hydrazine in water was added. The mixture was stirred at room temperature overnight. The nanospheres were then precipitated by centrifugation, separated from the supernatant, and rinsed with water. The nanospheres were rinsed three times. To minimize surface oxide formation on Pd, all solutions were degassed with argon and all operations were performed under an argon atmosphere.

Thermogravimetric Analysis. Thermogravimetric analysis (TGA) was performed with a Netzch (model STA 449C) instrument. Some 5 mg of sample was weighed into a sample boat. The sample was then placed along with an empty boat (as reference) into a furnace that was ramped up to 600 °C at 10 °C/min under a nitrogen atmosphere. Decreases in the weight of the sample due to polymer decomposition were monitored as a function of temperature.

Analysis of a pure nanosphere sample indicated that there was 86.5% weight loss between 150 and 500 °C due to polymer decomposition. This gave a weight ratio of 6.4 for the decomposed and carbonized fractions of the nanospheres. For pure $PdCl_2$, the weight loss was insignificant between 150 and 500 °C. If we assume that the same mass loss patterns are followed for $PdCl_2$ and the nanospheres in a $PdCl_2$-impregnated nanosphere sample, the mass loss, w_l, between 150 and 500 °C would be totally attributed to nanosphere decomposition. The $PdCl_2$ loading, defined as the mass of $PdCl_2$ loaded into unit gram of nanospheres, was obtained from $(w_0 - w_l - w_l/6.4)/(w_l + w_l/6.4)$, where w_0 is the initial mass of the sample.

Transmission Electron Microscopy and Electron Diffraction. TEM images were obtained using a Hitachi H-7000 instrument operated at 100 kV. TEM samples were obtained by aspirating a fine mist of a dilute solution (≈0.1 mg/mL) of the polymer nanospheres onto a carbon-coated copper grid using a home-built device.[20] The samples that contained no metal were then placed in a vial containing osmium tetraoxide (Aldrich) vapor for 4 h to stain the double bonds. TEM grids of the nanospheres containing palladium were not stained because the palladium was a suitable nucleus to scatter the electron beam.

Triethylallylammonium Bromide. Triethylallylammonium bromide (TEAA) was synthesized following a literature procedure.[21] To 200 mL of triethylamine (Aldrich) was added ≈30 mL of allyl bromide (Aldrich). The mixture was stirred for 48 h at room temperature and salt product formation was indicated by the appearance of a fine white precipitate. The slurry was then added to dry diethyl ether (Fisher) and stirred for 1 h. The precipitate was filtered and re-crystallized from methanol and diethyl ether.

Hydrogenation. The Pd nanoparticles were used to catalyze the hydrogenation of the following substrates: TEAA, vinylacetic acid (VAA, Aldrich), methyl methacrylate (MMA, Aldrich), and ethylene glycol dimethacrylate (EGDMA, Aldrich).

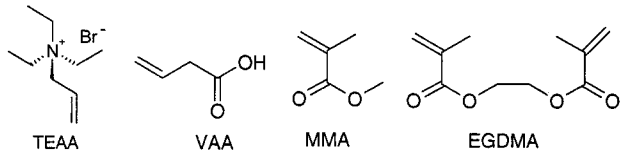

All of the reactions were performed at room temperature or 22 ± 2 °C using the same batch of nanospheres with a Pd loading of 0.17 g/g or 0.32 mol Pd per mol of carboxyl groups as the catalyst. The same batch was used, as the hydrogenation rate but not the trend changed somewhat from one to another batch of catalyst. Hydrogenation of TEAA was performed in D_2O and that of the other substrates was performed in methanol. In all cases, a fresh catalyst was used and the reactant/Pd molar ratio was controlled at 90:1. The setup for reaction was

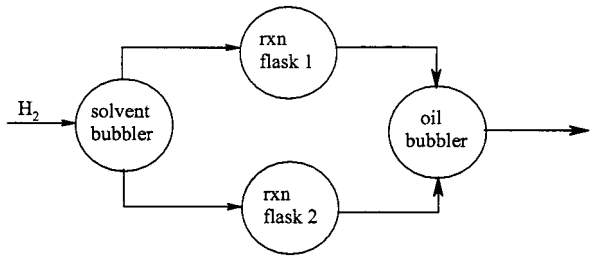

Hydrogen flowed at 0.5 mL/min into a methanol or D_2O bubbler and then into the reaction vessels. The bubbler was installed to minimize solvent loss from the reaction vessels. The hydrogen flow rate was optimized to minimize reactant loss due to evaporation but allow the replenishment of hydrogen to the surface of the Pd particles. The flow rate of 0.5 mL/min was chosen because a calculation based on the measured hydrogenation rate indicated that it was more than enough to replenish hydrogen loss in the vessels due to reaction. A control experiment in the absence of Pd suggested that an insignificant amount of MMA, which had the lowest boiling point among all tested substrates, was lost at such a hydrogen bubbling rate during the time span of interest. For each substrate, the reaction was performed in parallel at pH 3 and pH 10 in two vessels. The pH was adjusted using either 1 N HCl or solid NaOH. The concentrated base and acid were used to minimize the dilution of the reaction mixture.

In a typical experiment, ≈5 mg of nanospheres was dispersed in 5.0 mL of solvent. Hydrogen was bubbled through the solution for 30 min to reduce surface oxides to Pd.[22] The reactant was then added using a microsyringe in the case of liquid reactants. For the solid TEAA, the nanospheres were dissolved in 4 mL of D_2O and TEAA was dissolved in the remaining 1 mL of D_2O before its mixing with the catalyst.

To test for size selectivity, equal moles of MMA and EGDMA were combined in methanol. They were added to the reaction vessel so that the total moles of reactants were 90 times higher than that of the catalyst.

(8) Hirai, H.; Yakura, N.; Seta, Y.; Hodoshima, S. *React. Function. Polym.* **1998**, *37*, 121.
(9) Mayer, A. B. R.; Mark J. E. *Macromol. Rep.* **1996**, *A33*, 451.
(10) Ahmadi, T. S.; Wang, Z. L.; Green, T. C.; Henglein, A.; El-Sayed, M. A. *Science* **1996**, *272*, 1924.
(11) Jana, N. R.; Wang, Z. L.; Pal, T. *Langmuir* **2000**, *16*, 2457.
(12) Reetz, M. T.; Lohmer, G. *Chem. Commun.* **1996**, 1921.
(13) Schmid, G. *Chem. Rev.* **1992**, *92*, 1709.
(14) Lewis, L. N. *Chem. Rev.* **1993**, *93*, 2693.
(15) (a) Ciebien, J. F.; Cohen, R. E.; Duran, A. *Supramol. Sci.* **1998**, *5*, 31. (b) Ciebien, J. F.; Cohen, R. E.; Duran, A. *Mater. Sci. Eng.* **1999**, *7*, 45.
(16) Vorontsov, P. S.; Gerasimov, G. N.; Golubeva, E. N.; Grigor'ev, E. I.; Zav'yalov, S. A.; Zav'yalova, L. M.; Trakhtenberg, L. I. *Russ. J. Phys. Chem.* **1968**, *72*, 1742.
(17) Besoukhanova, C. B.; Guidot, J.; Barthomeuf, Breysse, M.; Bernard, J. R. *J. Chem. Soc., Faraday Trans. 1* **1981**, *77*, 1595.
(18) Plyuto, Y.; Berquier, J.-M.; Jacquiod, C.; Ricolleau, C. *Chem. Commun.* **1999**, 1653.
(19) Tago, T.; Hanaoka, T.; Dhupatemiya, P.; Hayashi, H.; Kishida, M.; Wakabayashi, K. *Catal. Lett.* **2000**, *64*, 27.
(20) Ding, J.; Liu, G. *Macromolecules* **1999**, *32*, 8413.
(21) Menger, F. M.; Venkataram, U. V. *J. Am. Chem. Soc.* **1986**, *108*, 2980.
(22) Borszeky, K.; Mallat, T.; Baiker, A. *Catal. Lett.* **1999**, *59*, 95.

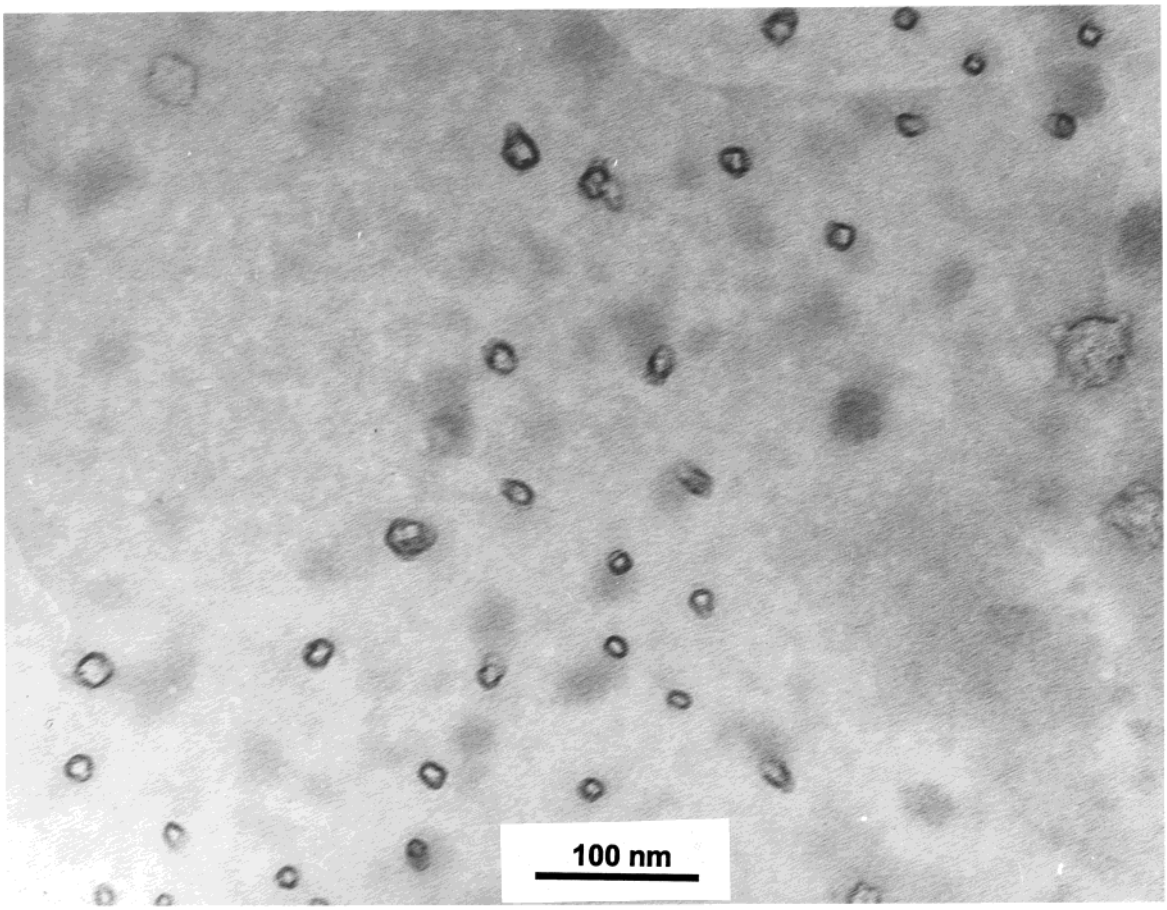

Figure 1. TEM images of PI-*b*-PCEMA-*b*-P*t*BA nanospheres after PCEMA cross-linking, PI hydroxylation, and removal of *tert*-butyl groups (stained with OsO_4 over a weekend).

For all but the TEAA reaction, aliquots, at ≈0.1 mL, were taken at different times for composition analysis. For the TEAA reaction, each aliquot consisted of ≈0.3 mL. The samples were centrifuged for 2.5 min at 5×10^3 rpm to separate the encapsulated catalyst from the alkene and product(s). The mixtures from MMA and EGDMA hydrogenation were analyzed by a gas chromatograph equipped with a mass spectrometer detector (GC/MS). For GC separation, a S.G.E. OV-101-coated fused silica capillary column was used. Compositions of the VAA hydrogenation mixture were analyzed using both ^{1}H NMR and GC/MS. In all GC/MS analyses, butanol was added as an internal standard. The GC/MS analysis error as checked from multiple analysis of the same sample was <3%.

The progress of TEAA hydrogenation was monitored using NMR. The decrease in the intensities of the vinylic proton peaks relative to those of the ethyl protons was used to follow TEAA disappearance.

In several control experiments, Pd black (Aldrich, specific surface area = 40 m^2/g) was used as the hydrogenation catalyst. The experiments were performed under otherwise the same conditions with a reactant-to-Pd molar ratio of 100:1.

Results and Discussion

PHI-*b*-PCEMA-*b*-PAA Nanospheres. The nanospheres were derivatized from polyisoprene-*block*-poly(2-cinnamoyloxyethyl methacrylate)-*block*-poly(*tert*-butyl acrylate) or PI-*b*-PCEMA-*b*-P*t*BA.[23] The precursor to PI-*b*-PCEMA-*b*-P*t*BA was prepared by anionic polymerization. Thus, the triblock used had narrow molar mass distribution with $\bar{M}_w/\bar{M}_n = 1.16$. Light scattering and NMR analysis revealed that the triblock consisted of 370 isoprene, 420 CEMA, and 550 *t*BA units.

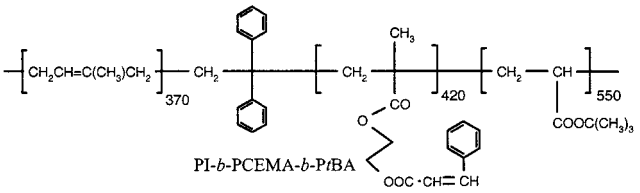

Micelles of PI-*b*-PCEMA-*b*-P*t*BA were prepared in THF/hexane with 65%, by volume, of hexane. Such micelles had PI coronas, insoluble PCEMA shells, and P*t*BA cores. The structure of the micelles was locked in by photo-cross-linking the PCEMA shells to yield nanospheres. The nanospheres were made water-dispersible by adding two hydroxyl groups across a double bond of an isoprene unit. The core block was converted into poly(acrylic acid) by removing the *tert*-butyl groups of P*t*BA via hydrolysis.[1] Illustrated in Figure 1 is a TEM image of the nanospheres with PHI coronas, cross-linked PCEMA shells, and PAA cores. The particles appear void because they were stained with OsO_4, which stained the PCEMA shells only. The average diameter of the light PAA cores is ≈16 nm. In water, the overall diameter of the particles, including the water-soluble PHI coronas, was 89 nm as determined from dynamic light scattering. The conversion of PCEMA double bonds after photolysis was 40%.

(23) Stewart, S.; Liu, G. *Chem. Mater.* **1999**, *11*, 1048.

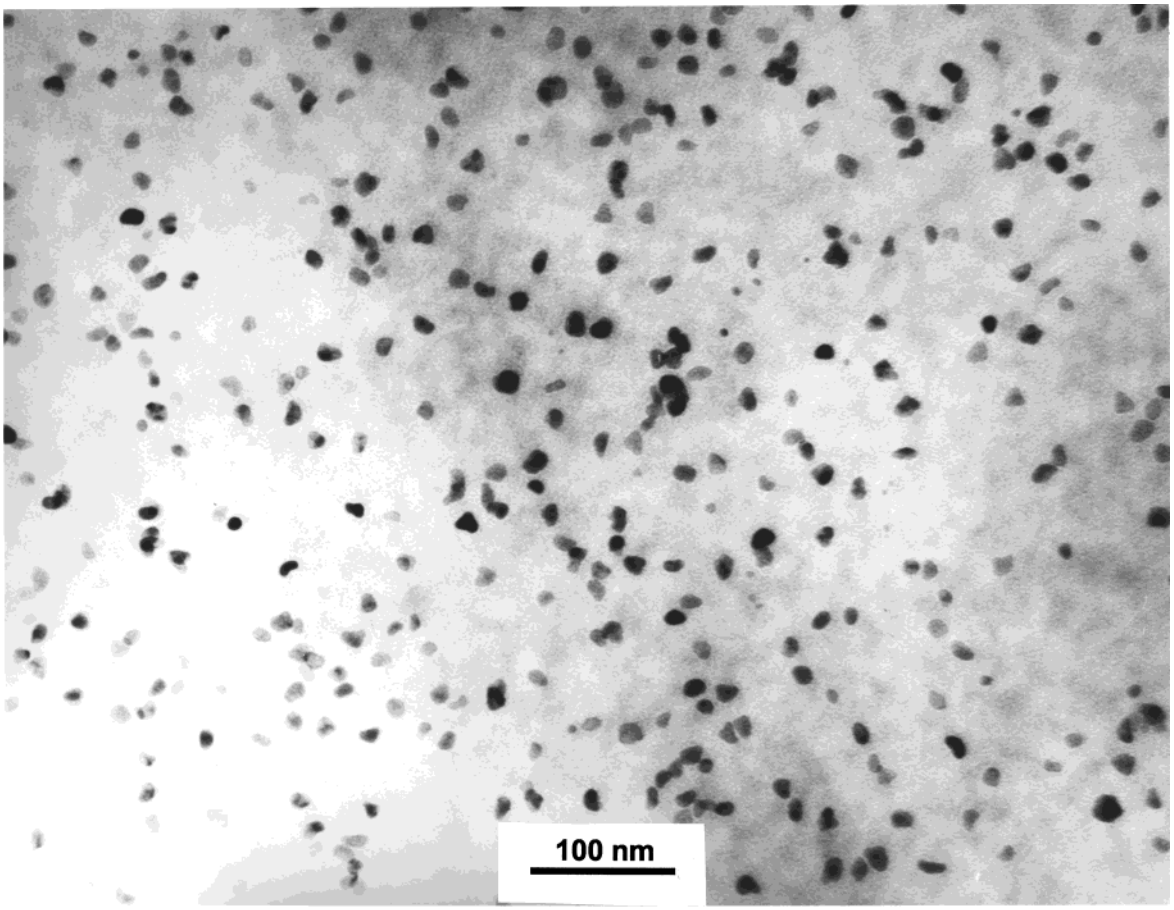

Figure 2. TEM images of PI-*b*-PCEMA-*b*-P*t*BA nanospheres after Pd loading (no staining).

Table 1. Comparison between the Literature and Experimental d_{hkl} Spacings of the Pd Nanoparticles

d_{hkl}/nm (exptl)	d_{hkl}/nm (literature)[25]	Miller indices
0.224	0.224	111
0.192	0.195	200
0.135	0.138	220
0.114	0.112	222

Pd Particle Formation. Pd^{2+} enters the PAA cores due to complexation with the AA groups.[24] The complexed Pd^{2+} was then reduced by hydrazine according to the following reaction:

$$2Pd^{2+} + H_2NNH_2 \rightarrow 2Pd + N_2\uparrow + 4H^+ \qquad (1)$$

The morphology of the formed Pd particles is shown in the TEM image of Figure 2. Because the specimen was not stained, the dark regions represent projections of the Pd particles. The majority of the particles are not spherical. Regardless of their shape, the largest dimension of the particles is less than ≈15 nm, the diameter of the nanosphere cores. Thus, the particles were prepared by template synthesis or inside the cores.

The preparation of Pd particles was confirmed by an electron diffraction experiment. By comparing the radii of the diffraction halos of the Pd particles with those of gold, we obtained the d_{hkl} values for the sample as shown in Table 1. The agreement between our d_{hkl} values and the literature values[25] is excellent and so is the comparison between the relative intensities of the different halos and those reported for Pd.

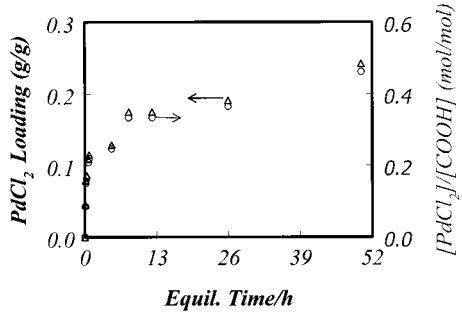

Figure 3. Plot of variation in $PdCl_2$ loading as a function of time of equilibration between $PdCl_2$ and the nanospheres in methanol.

Kinetics of $PdCl_2$ Loading. The kinetics of $PdCl_2$ loading into the cores of the nanospheres was followed by TGA as described in the Experimental Section. Shown in Figure 3 are the results in terms of grams of $PdCl_2$ incorporated into each gram of nanospheres or moles of $PdCl_2$ complexed with each mole of acrylic acid groups. $PdCl_2$ loading increased initially steeply with equilibration time and reached 0.109 g/g or 0.165 mol/mol in 40 min. The loading increased to ≈0.242 g/g or 0.46 mol/mol at 50 h. The loading of 0.46 mol/mol is very close to the theoretical maximum of 1/2 mol/mol, at

(24) Stephenson, T. A.; Morehouse, S. M.; Powell, A. R.; Heffer, J. P.; Wilkinson, G. **1965**, 3632.

(25) Joint Committee on Powder Diffraction. *Mineral Powder Diffraction File Data Book*; PA, 1980; Vol. 1.

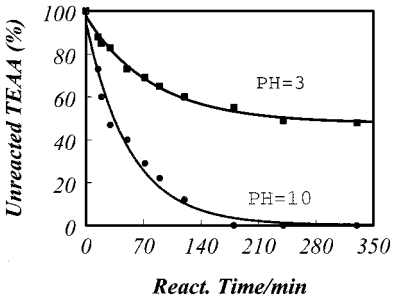

Figure 4. Decrease in the normalized concentration of TEAA, c/c_0, as a function of time at pH = 3 and pH = 10 in D_2O, when nanosphere-encapsulated Pd was used as the catalyst. The initial TEAA-to-Pd molar ratio was 90.

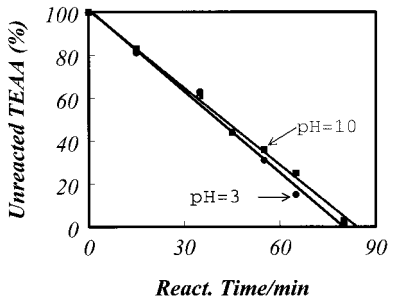

Figure 5. Decrease in the normalized concentration of TEAA, c/c_0, as a function of time at pH = 3 and pH = 10 in D_2O when Pd black was used as the catalyst. The initial TEAA-to-Pd molar ratio was 100.

which two carboxyl groups complex with one Pd ion. Thus, the efficiency of Pd loading was high.

We also performed TGA analysis of nanosphere-encapsulated Pd particles. After equilibrating the nanospheres for 24 h with $PdCl_2$ and reducing $PdCl_2$ overnight with hydrazine, we obtained a Pd loading of 0.16 g/g. This procedure was repeated once and twice and the Pd loading increased to 0.17 and 0.18 g/g, respectively.

Hydrogenation of TEAA. One of the presumed advantages of the nanosphere-encapsulated Pd particles was that we could modify the activity of the catalyst by changing the encapsulating environments of the Pd particles. The AA groups of the cores have $pK_a \approx 5.7$.[26,27] The AA groups would thus be fully protonated at low pHs and deprotonated at high pHs. To check how the charge density change in the core with pH would affect the rate of hydrogenation, we used a charged alkene, TEAA, as the substrate.

Illustrated in Figure 4 is the comparison of the hydrogenation results of TEAA at pH = 3 and pH = 10. The reaction went to completion at pH = 10 in ~3 h. The reaction rate at pH = 3 was slower and could not go to completion. Illustrated in Figure 5 is the comparison of the hydrogenation results of TEAA at pH = 3 and pH = 10 using Pd black as the catalyst. Within experimental error, hydrogenation kinetics in this case was independent of pH. Thus, the observed activity change of our Pd particles must have resulted from structural changes in the encapsulating nanospheres. The hydrogenation rate increased at pH = 10 most likely because the negatively charged AA groups at this pH attracted the positively charged TEAA.

A closer examination of Figures 4 and 5 revealed that different kinetic laws were followed for TEAA hydrogenation catalyzed by our Pd particles and Pd black. The hydrogenation kinetics catalyzed by Pd black had zero-order dependence on TEAA concentration. The solid lines in Figure 4 represent the best fit to the kinetic data by

$$\frac{C}{C_0} = a + b \exp(-t/\tau_{app}) \qquad (2)$$

At pH = 10, $a = 0.002$, $b = 0.949$, and $\tau_{app} = 53.5$ min. These suggested that the kinetics was first-order with respect to TEAA. Fitting the kinetic data at pH = 3 using eq 3 yielded $\tau_{app} = 81.4$ min, $a = 0.477$, and $b = 0.499$. The larger τ_{app} value at pH = 3 than that at pH = 10 was in agreement with a slower reaction at pH = 3. The more drastic aspect had been that the a and b values were not typical of irreversible first-order reactions but suggested either the establishment of an equilibrium or the shutdown of the reaction pathway at higher conversions.

Despite the totally different pathways for the reaction catalyzed by Pd black and nanosphere-encapsulated Pd, the reactant and product were the same and the thermodynamic equilibrium would not be affected by the use of different catalysts. Because the reaction went to completion when Pd black was used, the kinetic data of Figure 4 at pH = 3 could not be justified by the establishment of equilibrium. The stopping of the reaction at a certain conversion must be due to the shutdown of the reaction pathway probably because of catalytic surface covering by side products or polymer chains at pH = 3.

Kinetic Models for TEAA Hydrogenation. To justify qualitatively the different kinetic laws followed by the hydrogenation catalyzed by Pd black and our particles and to gain better insight into the kinetic data, kinetic models will be invoked next. For simplicity, we assume the absence of catalyst poisoning despite the fact that it must have happened at pH = 3 for hydrogenation catalyzed by the encapsulated Pd particles. We further assume that the PHI coronas are solvent-swollen and thus the reagents diffuse through them without much resistance. On the basis of these assumptions, the pathway for a reaction to occur would involve

$$R_{1B} \underset{k_{-11}}{\overset{k_{11}}{\rightleftharpoons}} R_{1S} \qquad (3a)$$

$$R_{1S} \underset{k_{-12}}{\overset{k_{12}}{\rightleftharpoons}} R_{1C} \qquad (3b)$$

$$R_{1C} + Pd \underset{k_{-13}}{\overset{k_{13}}{\rightleftharpoons}} R_1{-}Pd \qquad (3c)$$

$$R_1{-}Pd \xrightarrow[k_{14}]{H} \text{- - -}\rightarrow \qquad (3d)$$

where step (a) denotes the partition of the reactant R_1 between the bulk (B) and nanosphere PCEMA shell (S), step (b) the partition of the reactant between the PCEMA shell and PAA core (C), step (c) the partition

(26) Mark, H. F.; Bikales, N. M.; Overberger, C. G.; Menges, G. *Encyclopedia of Polymer Science and Technology*, 2nd ed.; Intersciences: New York, 1985; Vol. 1, p 228.

(27) Liu, G.; Guillet, J. E.; Al-Takrity, E. T. B.; Jenkins, A. D.; Walton, D. R. M. *Macromolecules* **1991**, *24*, 68.

of the reactant between the PAA core and the Pd surface, and step (d) the reaction occurring on the Pd surface between a H atom and R_1. The reaction is assumed irreversible because it has been shown to go to completion on Pd black surfaces. The dashed arrow in step (d) implies the omission of steps involving (e) product partition between the Pd surface and the PAA core, (f) the partition of the product between the PAA and PCEMA phases, and (g) the partition of the product between the PCEMA and bulk phases. Steps (e), (f), and (g) are assumed irreversible and fast compared to the first steps. This may be reasonable because a hydrogenated hydrocarbon does not contain a double bond and does not adsorb to the Pd surfaces. Once the drive for chemical adsorption is lost, the product would diffuse rapidly into the bulk, which is a good solvent for the product. This assumption is further justified by the consideration that our objective is not for a quantitative theory but for a glimpse of the intricate play of the different factors in the system.

The kinetic equations for the above reactions are

$$\frac{d[R_{1S}]}{dt} = k_{11}[R_{1B}] - k_{-11}[R_{1S}] - k_{12}[R_{1S}] + k_{-12}[R_{1C}] \quad (4a)$$

$$\frac{d[R_{1C}]}{dt} = k_{12}[R_{1S}] - k_{-12}[R_{1C}] - k_{13}[R_{1C}](1 - \theta_1) + k_{-13}\theta_1 \quad (4b)$$

$$\frac{d\theta_1}{dt} = k_{13}[R_{1C}](1 - \theta_1) - k_{-13}\theta_1 - k_{14}'\theta_1 \quad (4c)$$

$$\frac{d[P]}{dt} = k_{14}'\theta_1 \quad (4d)$$

where

$$k_{14}' = k_{14}\theta_H \quad (5)$$

In setting up eqs 4b, 4c, and 4d, reactant 1 (R_1) and H atoms were assumed to occupy different types of surface sites[28] so that θ_1 and $1 - \theta_1$ gave the fractions of occupied and unoccupied sites for R_1, respectively. Because of the fast bubbling of H_2 and the much faster diffusion of H_2 relative to R_1, the surface coverage by hydrogen atoms, θ_H, was assumed constant throughout the experiment. Making steady-state approximations with respect to $[R_{1S}]$, $[R_{1C}]$, and θ_1 and assuming that $K_{13}[R_{1C}] \ll (1 + k_{14}'/k_{-13})$, we obtained

$$-\frac{d[R_{1B}]}{dt} = k_{app}[R_{1B}] \quad (6)$$

with

$$k_{app} = k_{14}' \frac{K_{13}}{(1 + k_{14}'/k_{-13})\left[\frac{1}{K_{11}K_{12}} + (k_{14}'/k_{11} + k_{14}'/(k_{12}K_{11}))\frac{K_{13}}{1 + k_{14}'/k_{-13}}\right]} \quad (7)$$

In eq 7, K_{11}, K_{12}, and K_{13} are the partition coefficients for steps (4a), (4b), and (4c), respectively, and they are the ratios of forward to backward reaction rate constants.

Despite its inability to explain the stopping of reaction at pH = 3, eq 6 clearly suggests that the reaction is first-order. Upon changing the pH from 3 to 10, k_{14}' would not have changed, as we did not see a pH effect on the rate of Pd black catalyzed hydrogenation. Neither would k_{11} or K_{11} change dramatically because the structural change of the PCEMA shell would be small. We do not think that there is a drastic change in K_{13} or k_{-13} with pH change because Pd is in contact with the PAA layer. By going from the bulk of PAA to the interface of PAA and Pd, TEAA does not lose much of the favorable electrostatic interaction energy as it does from the core to the PCEMA shell. The reason for an increase in the rate of reaction from pH 3 to pH 10 was because of a drastic increase in K_{12} and k_{12}.

For hydrogenation catalyzed by Pd black, the kinetics was simpler without involving steps (3a) and (3b). The rate-determining step was the combination between an adsorbed hydrogen atom and an adsorbed allyl double bond[29]

$$-\frac{d[R_1]}{dt} = k\theta_H\theta_1 \quad (8)$$

where

$$\theta_1 = \frac{K[R_1]}{1 + K[R_1]} \quad (9)$$

The parameter K in eq 9 is the coefficient of TEAA partition between the bulk and Pd surfaces. Because alkenes were adsorbed strongly by Pd, $K[R_1] \gg 1$ and $\theta_1 \rightarrow 1$. Thus, the reaction rate had zero-order dependence on TEAA concentration.

Practical Aspects of TEAA Hydrogenation. Despite the totally different pathways for hydrogenation catalyzed by Pd black and the encapsulated Pd, the time taken for the quantitative conversion of TEAA at pH = 10 was comparable in the two cases, being ≈80 min for the former and ≈180 min for the latter. Thus, the use of the encapsulated Pd is practical as far as reaction rate is concerned.

The difference in reaction rates in the two cases could be due to the diffusion barrier created by the encapsulating layer or caused by the different specific surface areas for the two catalysts. Aldrich provided a specific surface area of 40 m^2/g for the Pd black. The TEM image of Figure 2 gives an approximate radius of 5 nm for the Pd particles. Because the density of Pd is 12 g/cm,[30]

(28) Gates, B. C. *Catalytic Chemistry*; Wiley & Sons: New York, 1992; p 376.

(29) Atkins, P. *Physical Chemistry*, 6th ed.; Freeman and Co: New York, 1997; Chapter 28, p 866.

(30) Lide D. R. *Handbook of Chemistry and Physics 76th Ed.*; CRC Press: Boca Raton, FL, 1995; pp 4−75.

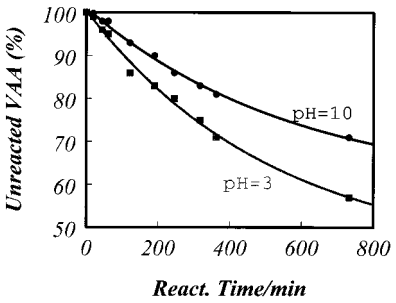

Figure 6. Decrease in the normalized concentration of VAA, c/c_0, as a function of time at pH = 3 and pH = 10 in methanol when nanosphere-encapsulated Pd was used as the catalyst. The initial VAA-to-Pd molar ratio was 90.

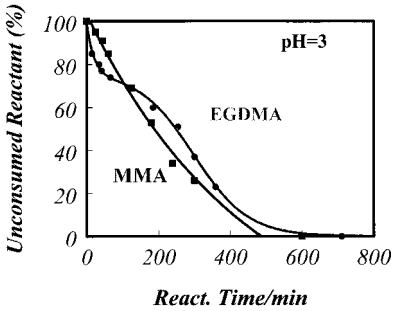

Figure 7. Comparison of MMA and EGDMA consumption data at pH = 3 in methanol when nanosphere-encapsulated Pd was used as the catalyst. The reactions were performed separately for each of the reactants. The initial MMA- or EGDMA-to-Pd molar ratio was 90.

we obtain a specific surface area of 50 m^2/g for the encapsulated Pd particles using this radius. Thus, the main cause for this reaction slowing down when the encapsulated Pd was used should be the diffusion barrier created by the encapsulating layer.

Hydrogenation of VAA. The structural change of the nanospheres due to pH change affected the rate of TEAA hydrogenation. If core charge density change was mainly responsible for this, we should see an opposite effect if a negatively charged alkene was used. To test this, we used VAA, which was negatively charged at pH = 10 but neutral at pH = 3.

Illustrated in Figure 6 were hydrogenation kinetic results for VAA at the two different pHs. Fitting the experimental data with eq 3 yielded $a = 0.429$, $b = 0.575$, and $\tau_{app} = 523$ min at pH = 3 and $a = 0.598$, $b = 0.421$, and $\tau_{app} = 578$ min at pH = 10. Thus, the reaction was disfavored at pH = 10, in agreement with our prediction. Unfortunately, the reaction did not seem to go to completion at either pH, presumably due to catalyst poisoning.

Hydrogenation of MMA and EGDMA. The other presumed advantage of the encapsulating layer was that it might function as a nanofilter, just as the outer layer of a dendrimer does.[31] The nanofilter selects the smaller reactant for hydrogenation. For testing this, we studied the hydrogenation of MMA and EGDMA, where EGDMA was twice as large as MMA.

Presented in Figures 7 and 8 is the comparison between the data of MMA and EGDMA consumption at pH = 3 and pH = 10, respectively, when the reaction

(31) Bosman, A. W.; Janssen, H. M.; Meijer, E. W. *Chem. Rev.* **1999**, *99*, 1665.

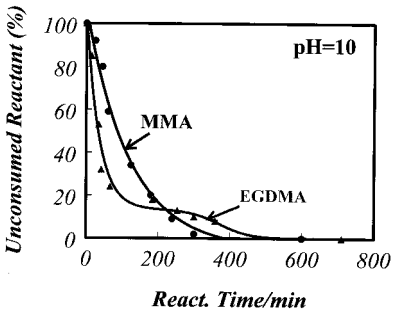

Figure 8. Comparison of MMA and EGDMA consumption data at pH = 10 in methanol when nanosphere-encapsulated Pd was used as the catalyst. The reactions were performed separately for each of the reactants. The initial MMA- or EGDMA-to-Pd molar ratio was 90.

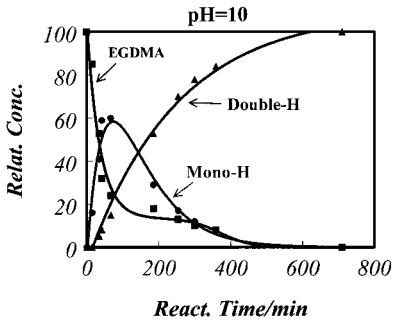

Figure 9. Product distribution for EGDMA hydrogenation at pH = 10 at different times.

was done separately for each of the reactants. The general trend seemed to be that EGDMA reacted faster than MMA at low conversions but slower at high conversions. Thus, we do not see a clear-cut nanofilter effect.

The missing of a clear-cut nanofilter effect could be easily appreciated from eqs 7 and 8. The apparent rate constant was a complex function of the rate constants of the various steps shown in eq 3. EGDMA might have smaller k_{11} and k_{12} values, which decreased k_{app}. This effect could, however, be offset by a larger K_{13}. The reaction could be more favorable for EGDMA at low conversions due to a larger adsorption equilibrium constant K_{13}. K_{13} was larger for EGDMA because it contained two rather than one double bond. Thus, the lack of the nanofilter effect was most likely due to the fact that we used EGDMA rather than mono-hydrogenated EGDMA in this comparative study.

The reaction rate of EGDMA slowed relative to that of MMA at higher conversions presumably due to the fact that mono-hydrogenated EGDMA, EGDMA$-H_2$, formed as an intermediate competed with EGDMA for surface adsorption sites for further hydrogenation to the fully hydrogenated product, EGDMA$-H_4$. Illustrated in Figure 9 were the variations in EGDMA, EGDMA$-H_2$, and EGDMA$-H_4$ relative concentrations as a function of time for EGDMA hydrogenation at pH = 10. The building up of EGDMA$-H_2$ concentration at intermediate times was evident. It was also because of the effect of this competition between EGDMA and EGDMA$-H_2$ for surface sites that caused the nonexponential decay in the concentration of EGDMA.

Illustrated in Figure 10 was the comparison between the kinetics of MMA hydrogenation at pH = 3 and pH = 10, respectively. The reaction rate was higher at pH

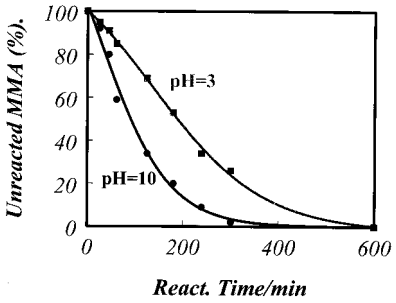

Figure 10. Comparison of MMA hydrogenation kinetic data in methanol at pH = 3 and pH = 10.

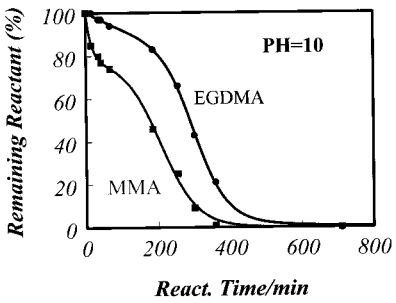

Figure 11. Comparison of MMA and EGDMA hydrogenation kinetic data at pH = 10 in methanol when nanosphere-encapsulated Pd was used as the catalyst. The reaction was performed for a mixture of MMA and EGDMA. The initial MMA-to-EGDMA-to-Pd molar ratios were 45:45:1.

= 10. A similar trend was found for EGDMA hydrogenation. This trend can again be justified qualitatively by eqs 6 and 7. Upon pH increase from 3 to 10, the cores became charged. This should not have affected K_{11}, k_{11}, and k_{14}' of eq 7 significantly. What were affected the most would be K_{12}, k_{12}, K_{13}, and k_{-13}. Because both MMA and EGDMA would be less soluble in the charged cores, K_{12}, k_{-13}, and k_{12} would be decreased relative to those at pH = 3 and K_{13} increased. The fact that the rate increased at pH = 10 suggested that the dominant effect in increasing pH was to increase K_{13}.

Hydrogenation of MMA and EGDMA Mixtures at pH = 10. The reactions discussed so far had all been performed individually with a single reactant. Selectivity in real situations would require the preferential reaction of a reactant in the presence of the other(s). Plotted in Figure 11 are the conversions of a MMA and EGDMA mixture initially at equal molar numbers as a function of time at pH = 10. Surprisingly, the kinetic curves looked so different from those shown in Figure 8. The concentration of neither MMA nor EGDMA decreased exponentially with time. Then, the nanofilter effect seemed to come in and MMA reacted preferentially at all times, in contrast to the trend observed in Figure 8.

The nonexponential decays of Figure 11 and those seen in Figures 8 and 9 for EGDMA concentration prompted us to obtain kinetic data using Pd black as the catalyst. Plotted in Figure 12 is the variation in the relative concentrations of MMA and EGDMA as a function of time from such a study. The nonexponential decay pattern was repeated for MMA using the Pd black catalyst. Although MMA reacted slightly faster than EGDMA, the selectivity of the catalyst was, however,

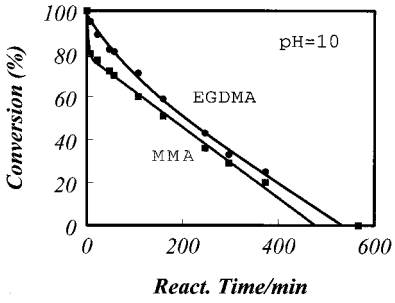

Figure 12. Comparison of MMA and EGDMA hydrogenation kinetic data at pH = 10 in methanol when Pd black was used as the catalyst. The reaction was performed for a mixture of MMA and EGDMA. The initial MMA-to-EGDMA-to-Pd molar ratios were 45:45:1.

not as good as what was shown by the encapsulated Pd particles.

The reason for the change in the concentration decay patterns of the reactants became apparent only after we had constructed a kinetic model for such a system. In a mixture, processes described by eqs 3a and 3b and thus rate laws by eqs 4a and 4b remained valid for reactants 1 and 2. The modification to eq 4c was

$$\frac{d\theta_1}{dt} = k_{13}[R_{1C}](1-\theta) - k_{-13}\theta_1 - k_{14}'\theta_1 \quad (10a)$$

$$\frac{d\theta_2}{dt} = k_{33}[R_{2C}](1-\theta) - k_{-23}\theta_2 - k_{24}'\theta_2 \quad (10b)$$

$$\theta_1 + \theta_2 = \theta \quad (10c)$$

Making steady-state approximations with respect to θ_1 and θ_2, we obtained the rates of reactants 1 and 2 disappearance in terms of $[R_{1C}]$ and $[R_{2C}]$:

$$-\frac{d[R_1]}{dt}\Big|_m = k_{14}'\frac{K_{13}[R_{1C}]}{K_{13}[R_{1C}] + 1 + k_{14}'/k_{13} + \dfrac{K_{23}[R_{2C}](1 + k_{14}'/k_{13})}{1 + k_{24}'/k_{23}}} \quad (11a)$$

$$-\frac{d[R_2]}{dt}\Big|_m = k_{24}'\frac{K_{23}[R_{2C}]}{K_{23}[R_{2C}] + 1 + k_{24}'/k_{23} + \dfrac{K_{13}[R_{1C}](1 + k_{24}'/k_{23})}{1 + k_{14}'/k_{13}}} \quad (11b)$$

The expressions for the hydrogenation rates of reactants reacting alone were obtained from setting $[R_{1C}] = 0$ for the hydrogenation of R_2 and $[R_{2C}] = 0$ for the hydrogenation of R_1.

$$-\frac{d[R_1]}{dt}\Big|_p = k_{14}'\frac{K_{13}[R_{1C}]}{K_{13}[R_{1C}] + 1 + k_{14}'/k_{13}} \quad (12a)$$

$$-\frac{d[R_2]}{dt}\Big|_p = k_{24}'\frac{K_{23}[R_{2C}]}{K_{23}[R_{2C}] + 1 + k_{24}'/k_{23}} \quad (12b)$$

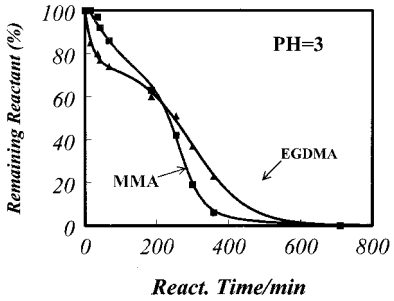

Figure 13. Comparison of MMA and EGDMA hydrogenation kinetic data at pH = 3 in methanol when nanosphere-encapsulated Pd was used as the catalyst. The reaction was performed for a mixture of MMA and EGDMA. The initial MMA-to-EGDMA-to-Pd molar ratios were 45:45:1.

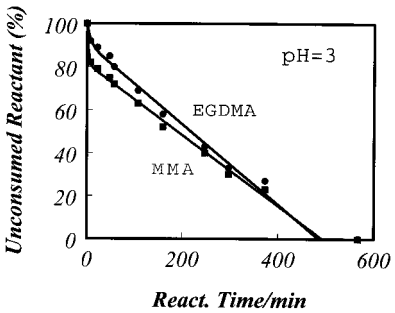

Figure 14. Comparison of MMA and EGDMA hydrogenation kinetic data at pH = 3 in methanol when Pd black was used as the catalyst. The reaction was performed for a mixture of MMA and EGDMA. The initial MMA-to-EGDMA-to-Pd molar ratios were 45:45:1.

Comparing eqs 11 and 12, it was not difficult to see why the kinetics could be so different when pure reactants and reactant mixtures were used. In the latter case, the consumption kinetics of the reactants was coupled. Unfortunately, we were not able to make quantitative predictions using eqs 11 and 10 because we did not solve eq 10 for the rate laws in terms of R_1 and R_2 bulk concentrations.

Hydrogenation of MMA and EGDMA Mixtures at pH = 3. We also performed the hydrogenation kinetics of MMA and EGDMA mixtures at pH = 3. Illustrated in Figures 13 and 14 are the data of MMA and EGDMA disappearance when the encapsulated Pd particles and Pd black were used as the catalyst. In the latter case, the kinetic data were essentially the same as those obtained at pH = 10, suggesting the pH insensitivity of the catalytic reactions. The data obtained using our nanoparticles as the catalyst suggested the absence of selectivity toward MMA at this pH. This was in agreement with data shown in Figure 7. The nonexponential concentration decay patterns here were again due to the appearance of $[R_{1C}]$ in rate equations for R_2 disappearance and vice versa.

Conclusion

We have prepared nanosphere-encapsulated Pd nanoparticles as confirmed by TEM and electron diffraction studies. Such Pd particles functioned as a hydrogenation catalyst as expected. The more interesting aspect has been in our ability to tune the activity of such Pd particles by changing the pH and thus the structures of the encapsulating nanospheres. Deprotonating the PAA core of the encapsulating spheres at pH = 10 increased the hydrogenation rate of a positively charged alkene TEAA. The hydrogenation rate of VAA decreased at pH = 10 because the depronatated PAA chains repelled the deprotonated VAA. When a mixture of MMA and EGDMA was hydrogenated at pH = 10, the encapsulating nanospheres functioned as a nanofilter and allowed the hydrogenation of the smaller MMA in preference to EGDMA. Kinetic models were proposed to provide some insight into the kinetic data.

Acknowledgment. NSERC of Canada is gratefully acknowledged for sponsoring this research. Sean Stewart is thanked for synthesizing and characterizing the PI-*b*-PCEMA-*b*-P*t*BA polymer. RU would like to thank NSERC, the Killam Foundation, and the University of Calgary for graduate scholarships and teaching assistantships.

CM0005743